

General Disclaimer

One or more of the Following Statements may affect this Document

- This document has been reproduced from the best copy furnished by the organizational source. It is being released in the interest of making available as much information as possible.
- This document may contain data, which exceeds the sheet parameters. It was furnished in this condition by the organizational source and is the best copy available.
- This document may contain tone-on-tone or color graphs, charts and/or pictures, which have been reproduced in black and white.
- This document is paginated as submitted by the original source.
- Portions of this document are not fully legible due to the historical nature of some of the material. However, it is the best reproduction available from the original submission.

NASA CR-11

144568

**SIDE LOOKING RADAR
CALIBRATION STUDY**

FINAL REPORT

Job Order 46-335

(NASA-CR-144568) **SIDE LOOKING RADAR
CALIBRATION STUDY Final Report (Lockheed
Electronics Co.) 46 F HC \$4.00 CSCL 17I**

N76-13332

**Unclas
G3/32 04839**

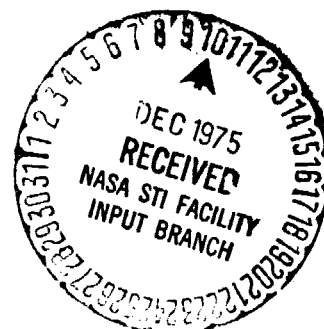
Prepared By

**Lockheed Electronics Company, Inc.
Aerospace Systems Division
Houston, Texas**

Contract NAS 9-12200

For

EXPERIMENTS SYSTEMS DIVISION



**National Aeronautics and Space Administration
LYNDON B. JOHNSON SPACE CENTER
Houston, Texas**

October 1975

**LEC-6242
Rev. A**

TECHNICAL REPORT INDEX/ABSTRACT
(See instructions on reverse side.)

1. TITLE AND SUBTITLE OF DOCUMENT

2. JSC NO.

JSC- 09714

**SIDE LOOKING RADAR CALIBRATION STUDY - FINAL REPORT
REV. A, DATED OCTOBER, 1975.**

3. CONTRACTOR/ORGANIZATION NAME

Lockheed Electronics Co., Inc.

4. CONTRACT OR GRANT NO.

NAS-9-12200

5. CONTRACTOR/ORIGINATOR DOCUMENT NO.

LEC-6242, Rev. A

6. PUBLICATION DATE (THIS ISSUE)

October 1975

7. SECURITY CLASSIFICATION

Unclassified

8. OPR (OFFICE OF PRIMARY RESPONSIBILITY)

T. K. Sampsel

9. LIMITATIONS

GOVERNMENT HAS UNLIMITED RIGHTS ☒ YES ☐ NO

10. AUTHOR(S)

**W. D. Edwards
Principal Engineer**

IF NO, STATE LIMITATIONS AND AUTHORITY

N/A

11. DOCUMENT CONTRACT REFERENCES

12. HARDWARE CONFIGURATION

WORK BREAKDOWN STRUCTURE NO.

N/A

SYSTEM

N/A

CONTRACT EXHIBIT NO.

N/A

SUBSYSTEM

N/A

DRL NO. AND REVISION

N/A

MAJOR EQUIPMENT GROUP

DRL LINE ITEM NO.

N/A

N/A

13. ABSTRACT

This report proposes that calibration of an Airborne Side Looking Radar can be accomplished by the use of a model that relates the radar parameters to the physical mapping situation. Discussion of such a radar model should include a description of the characteristics of the transmitters, the antennas, target absorption and reradiation, the receiver and map making or radar data processing and the calibration process.


14. SUBJECT TERMS

SIDE LOOKING RADAR
CALIBRATION STUDY

FINAL REPORT

Job Order 46-335


PREPARED BY


W. D. Edwards, Principal Engineer
Lockheed Electronics Company, Inc.


APPROVED BY

LEC

NASA


W. H. Beatty III, Supervisor
Sensor Systems Engineering
Section


R. Fenner, Head
Microwave Section


T. K. Sampsel, Chief
Sensor System Development
Branch

Prepared By
Lockheed Electronics Company, Inc.

For

Experiments Systems Division

NATIONAL AERONAUTICS AND SPACE ADMINISTRATION
LYNDON B. JOHNSON SPACE CENTER
HOUSTON, TEXAS

October 1975

LEC-6242
Rev. A

CONTENTS

Section	Page
1. INTRODUCTION.	1-1
2. TRANSMITTED PULSE	2-1
3. ANTENNA PATTERNS.	3-1
3.1 <u>ANTENNA AZIMUTHAL PATTERN.</u>	3-1
3.2 <u>ANTENNA PATTERN OF ELEVATION OR DEPRESSION ANGLES.</u>	3-1
4. GROUND RETURN	4-1
4.1 <u>MAPPING GEOMETRY</u>	4-1
4.2 <u>RADAR PULSE PACKET GEOMETRY.</u>	4-1
4.3 <u>BACK SCATTERING COEFFICIENT.</u>	4-5
5. TRANSFER FUNCTIONS.	5-1
5.1 <u>RECEIVER</u>	5-1
5.2 <u>RECORDER CRT</u>	5-1
5.3 <u>RECORDER DATA FILM</u>	5-3
5.4 <u>OPTICAL CORRELATOR/PROCESSOR</u>	5-5
5.5 <u>OUTPUT MAP FILM.</u>	5-5
5.6 <u>MICRODENSITOMETER.</u>	5-5
5.7 <u>ANALOG-TO-DIGITAL CONVERTER.</u>	5-8
5.8 <u>DIGITAL MAGNETIC TAPE RECORDING.</u>	5-8
6. COMPUTER DATA PROCESSING.	6-1
7. CALIBRATION METHODS	7-1
7.1 <u>SIMULATED TARGETS</u>	7-1
7.2 <u>CALIBRATION TEST RANGE</u>	7-2

Section	Page
7.2.1 DISTRIBUTED TARGET RESOLUTION.	7-2
7.2.2 SYSTEM DYNAMIC RANGE MEASUREMENT	7-3
7.2.3 PLANNING CONSIDERATIONS.	7-7
8. CONCLUSIONS	8-1
9. REFERENCES	9-1

FIGURES

Figure		Page
3-1	Antenna angle gain as a function of azimuthal angle.	3-2
4-1	Airborne side looking radar mapping geometry	4-2
4-2	Radar pulse packet geometry.	4-3
4-3	Terrain return data.	4-8
5-1	Transfer characteristics of elements in a coherent SLR system.	5-2
5-2	Typical optical correlator/processor	5-6
5-3	Typical system block diagram of SLR with optical processor.	5-7
7-1	Radar calibration test range	7-4

ABBREVIATIONS AND ACRONYMS

ADC	Analog-to-digital converter
CRT	Cathode ray tube
FM	Frequency modulation
LOS	Line-of-sight
MD	Microdensitometer
RPP	Radar pulse packet
SLR	Side looking radar
dc	Direct current
rf	Radio frequency

PRECEDING PAGE BLANK NOT FILMED

1. INTRODUCTION

This report, written for task order 46, job order 335, reports on a study to determine the methods and practicability of developing calibration techniques for Side Looking Radar (SLR) and fulfills the requirements of action document 46-335-C08. It is proposed that calibration of an airborne SLR can be accomplished by the use of a model that relates the radar parameters to the physical mapping situation. A discussion of a radar model should include a description of the characteristics of (1) the transmitter, (2) the antenna, (3) the target absorption and reradiation, (4) the receiver and map making or radar data processing, and (5) the calibration process.

2. TRANSMITTED PULSE

In order to achieve calibration, information on the transmitted pulse peak power, pulse shape, pulse width, pulse compression, and range side lobe level must be obtained. Depending on the type of processing used, perhaps spectral frequency information on the transmitted pulse will be necessary or desired. At any rate, a very accurate model or discrete description of the transmitted pulse must be obtained. This transmitted pulse information will be processed in the chain of information in succeeding sections of this report.

3. ANTENNA PATTERNS

3.1 ANTENNA AZIMUTHAL PATTERN

In any practical calibration scheme, the azimuthal pattern, whether real or synthetic, must be considered. A simple approach to a model is to assume an exponential model that can be used to represent the entire antenna pattern, such as the following equation

$$G(\phi) = G_0 e^{-k_1(\phi_1 - \phi_1)^2} + G_1 e^{-k_2(\phi_2 - \phi_{1/2})^2} \\ + G_2 e^{-k_3(\phi_3 - \phi_{1/2})^2} \dots + G_n e^{-k_n(\phi_n - \phi_{1/2})^2} \quad (3-1)$$

which creates a model as illustrated in figure 3-1. (The beam-width constants are the k's, and the lobe gains are the G's.) A more practical approach is to use measured pattern data that are a function of both azimuth and elevation. How the data should be processed will be discussed in a later section of this report.

3.2 ANTENNA PATTERN OF ELEVATION OR DEPRESSION ANGLES

To obtain equal power signals from identical reflectors in the ground plane, an airborne radar must have a "shaped" antenna pattern. The required pattern for obtaining the equal return signals is generally referred to as a $\csc^2 \cos^{1/2}$ function of an elevation or depression angle. This $\csc^2 \cos^{1/2}$ pattern can be obtained by reshaping a parabolic or a cylindrical reflector illuminated by a primary feed, usually a horn. The specific description of the required vertical antenna pattern depends

on the application of the radar; however, a selected example will be used to illustrate the specification of such a pattern. In general, the complete elevation pattern is specified in two parts by an exponential function and by a trigonometric function; i.e.,

$$G(\theta) = G_0 \left\{ e^{-P(\theta - \theta_0)^2} \Big|_{\theta_2}^{\theta_1} + P \csc^2 \theta \cos^{1/2} \theta \Big|_{\theta_3}^{\theta_2} \right\}. \quad (3-2)$$

To illustrate a practical case, consider an airborne antenna 0.5 meter in height by 2 meters in length operating at an altitude of 50,000 feet. Also, consider the maximum mapping range to be 500,000 feet and the operating frequency to be 10 GHz. Calculations on the vertical antenna pattern are made as follows:

Step 1 - Initial depression angle, θ_0

$$\theta_0 = \tan^{-1} \frac{50,000}{500,000} = 5.8^\circ = 0.101 \text{ rad} \quad (3-3)$$

Step 2 - Half-power beamwidth, β

$$\beta = \frac{1.2\lambda}{a} \quad (3-4)$$

where λ is the radiated wavelength and a is the vertical antenna aperture size:

$$\beta = \frac{(1.2)(3)}{50} = 0.072 \text{ rad}$$

$$= 4.13^\circ \quad (3-5)$$

Step 3 - Determination of the beamwidth constant p for the exponential portion of the pattern:

$$G(\theta) = e^{-p(\theta - \theta_0)^2} \Big|_{\theta_2}^{\theta_1} \quad (3-6)$$

From equations (3-3) to (3-6), one can observe that maximum gain occurs at the angle θ_0 and decreases exponentially on either side of the angle θ_0 . At an angle $\pm|\beta/2|$ from θ_0 , the one-way power level of the pattern is approximately 3 decibels below that of the angle θ_0 . By knowing these quantities, one can determine the value of p in equation (3-6) as follows:

$$G(\theta) \Big|_{\theta_0 - \theta_{1/2}} = e^{-p(\theta_0 - \theta_{1/2} - \theta_0)^2}$$

$$10 \log G(\theta) \Big|_{\theta_0 - \theta_{1/2}} = 10 \log e^{-p(\theta_{1/2})^2} = 3.0103 \text{ dB}$$

$$\log G(\theta) \Big|_{\theta_0 - \theta_{1/2}} = -p(\theta_{1/2})^2 \log e = 0.30103 \quad (3-7)$$

or

$$\begin{aligned}
 p &= \frac{0.30103}{(\theta_{1/2})^2 \log e} \\
 &= \frac{0.30103}{(\theta/2)^2 (0.43429)} \\
 &= \frac{0.30103}{(0.036)^2 (0.43429)} \\
 &= \frac{3.0103 \times 10^{-1}}{(1.29 \times 10^{-3})(4.3429 \times 10^{-1})} = 535 \quad (3-8)
 \end{aligned}$$

Step 4 - Determination of junction angle, θ_2

At the junction angle, θ_2 , the gain slopes are equal on a log curve; i.e.,

If

$$G_1(\theta) = e^{-p(\theta - \theta_0)} \quad (3-9)$$

and

$$G_2(\theta) = P \csc^2 \theta \cos^{1/2} \theta \quad (3-10)$$

then

$$\begin{aligned}
 \frac{d[\ln G_1(\theta_2)]}{d\theta} &= \frac{d}{d\theta}[\ln G_2(\theta_2)] \\
 " &= \frac{d}{d\theta} \left[\ln e^{-p(\theta_2 - \theta_0)^2} \right] \\
 " &= -2p(\theta_2 - \theta_0)
 \end{aligned} \tag{3-11}$$

and

$$\begin{aligned}
 \frac{d}{d\theta}[\ln G_2(\theta_2)] &= \frac{d}{d\theta}[\ln p + 2 \ln \csc \theta_2 \\
 &\quad + 1/2 \ln \cos \theta] \\
 " &= 0 + \frac{2}{\csc \theta_2}(-\csc \theta_2 \cot \theta_2) \\
 &\quad + \frac{1}{2} \frac{1}{\cos \theta_2}(-\sin \theta_2) \\
 " &= -2 \cot \theta_2 - \frac{1}{2 \cot \theta_2}
 \end{aligned} \tag{3-12}$$

or

$$\begin{aligned}
 2p(\theta_2 - \theta_0) &= 2 \cot \theta_2 + \frac{1}{2 \cot \theta_2} \\
 \theta_2 - \theta_0 &= \frac{\cot \theta_2}{p} + \frac{1}{4p \cot \theta_2} \\
 (\theta_2 - 0.101) &= \frac{\cot \theta_2}{535} + \frac{1}{2140 \cot \theta_2}
 \end{aligned} \tag{3-13}$$

From a trial-and-error solution, $\theta_2 \cong 6.7^\circ \cong 0.117$ rad.

Step 5 - Determination of the constant P for the $\csc^2 \theta \cos^{1/2} \theta$ function at θ_2 ,
 where $G_1(\theta) = G_2(\theta)$

$$\begin{aligned}
 P &= \frac{e^{-p(\theta_2 - \theta_0)^2}}{\csc^2 \theta_2 \cos^{1/2} \theta_2} \\
 &= \frac{e^{-535(0.117 - 0.101)^2}}{(8.58)^2 \sqrt{0.993}} \\
 &= \frac{e^{-0.137}}{73.5} = \frac{0.874}{73.5} = 0.019 \quad (3-14)
 \end{aligned}$$

Step 6 - Determination of G_0 , the maximum aperture gain

$$G_0 = \frac{4\pi \rho_a A}{\lambda^2} \quad (3-15)$$

where λ is the wavelength,

A is the physical area of the antenna, and

ρ_a is the antenna aperture efficiency
 (65 percent assumed).

$$\begin{aligned}
 G_0 &= \frac{4\pi(0.65)(0.5 \times 2)\text{m}^2}{(0.03)^2 \text{m}^2} \\
 &= 9060 \text{ or } 39.5 \text{ dB} \quad (3-16)
 \end{aligned}$$

Step 7 - The total theoretical description of the vertical pattern is then

$$G(\theta) = 9060 \left\{ e^{-535(\theta - 0.101)^2} \left| \begin{array}{l} 0.0084 \\ 0.117 \end{array} \right. + 0.019 \csc^2 \theta \cos^{1/2} \theta \left| \begin{array}{l} 6.7^\circ \\ 70^\circ \end{array} \right. \right\} \quad (3-17)$$

Some comments on the preceding vertical pattern description based on both theoretical and measured patterns include the following:

- A. The exponential portion of the pattern is specified starting at 0.48 degree, the -20-decibel power level of the one-way power pattern. This is an arbitrary choice of gain level.
- B. The 70-degree angle, the greatest depression angle, is also arbitrarily chosen. What the actual choice of the maximum depression angle is depends on the required range resolution as discussed in another section; i.e., $c\tau/2 \sec \theta$. Beyond the maximum specified depression angle, the power pattern should decrease as rapidly as is practical.
- C. Any deviations of the actual power pattern from the theoretical power distribution will result in an uneven ground illumination. Two-way propagation will result in further unequal return signal levels from similar terrain. For accurate calibration of an SLR, the actual antenna pattern must be measured and the power levels versus angle stored for subsequent data processing.

4. GROUND RETURN

4.1 MAPPING GEOMETRY

The geometrical situation of a mapping, airborne SLR is shown in figure 4-1. The reflecting area is a function of the radar parameters, the vector directions, and the target characteristics.

The scattering cross section per unit area is the projected area along the radar line-of-sight (LOS) determined by the radar pulse width, τ , and the antenna azimuthal beamwidth, ϕ . The use of τ and ϕ defines an area illuminated for a duration of $c\tau/2$, where c is the velocity of light and the 2 in the denominator accounts for the two-way radar energy transmission. The use of τ and ϕ can also be used to define a "pulse packet."

4.2 RADAR PULSE PACKET GEOMETRY

The geometrical situation of the terrain relative to the "radar pulse packet" is shown in figure 4-2. By use of the radar pulse packet and the antenna pattern beamwidth, a radar resolution cell in the ground plane can be described. The radar pulse packet (RPP) is an area in the ground plane bounded by the azimuthal dimension ($R_s \phi$) and the cross-track dimension ($\frac{c\tau}{2} \sec \theta$) i.e.,

$$RPP = (R_s \phi) \left(\frac{c\tau}{2} \sec \theta \right) \quad (4-1)$$

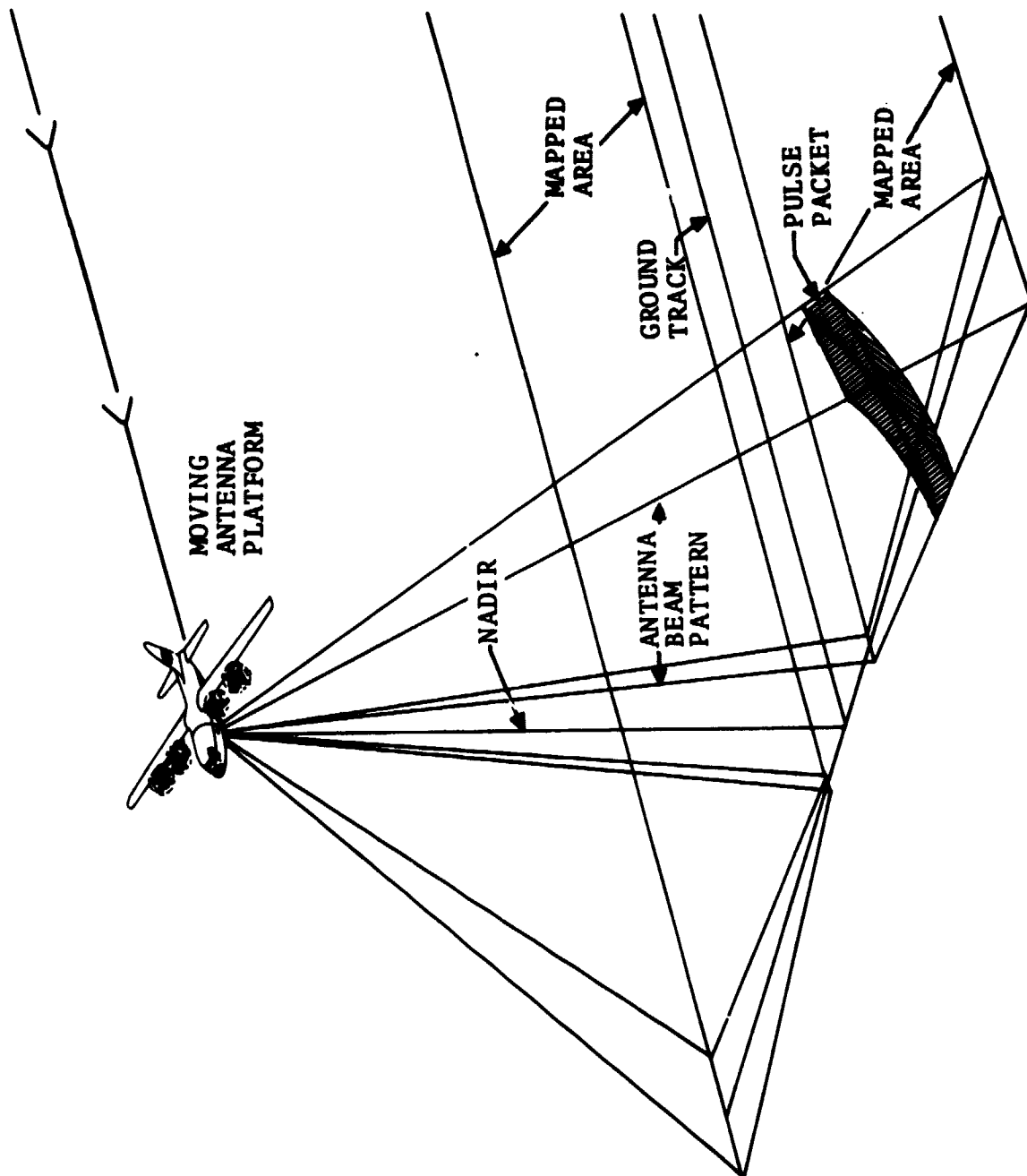


Figure 4-1. - Airborne side looking radar mapping geometry.

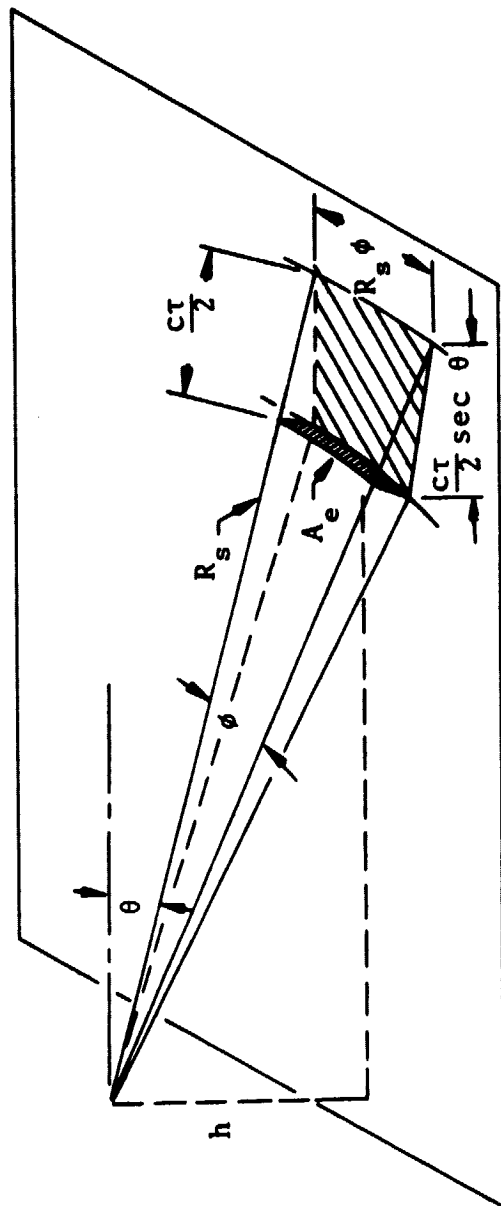


Figure 4-2. - Radar pulse packet geometry.

where

R_s is the slant range to a ground area

ϕ is the azimuth beamwidth in radians

c is the velocity of light

τ is the radar pulse width, and

θ is the depression angle from the horizontal.

The effective ground area, A_e , which is "seen" by the radar is the projection of the pulse packet perpendicular to the line-of-sight or,

$$A_e = (R_s \phi) \left(\frac{c\tau}{2} \tan \theta \right) \quad (4-2)$$

Although the effective ground area within a resolution cell can be described by equation (4-2), the electromagnetic characteristics of the material within the cell will determine the quantity of incident energy reradiated in the direction of the radar. That is, the resolution cell can be considered to contain individual radiators (such as dipoles) that can be used to describe the electromagnetic characteristics of various terrain types. Exact modeling of various terrain types is a monumental task as Moore points out (ref. 1) when he infers the magnitude of modeling a forest down to the leaf and pine-needle level. Moore further points out the lack of adequate scattering information and cites limited programs by the Massachusetts Institute of Technology (MIT) Radiation Laboratory (ref. 2), Philco Corporation (ref. 3), Goodyear Aerospace Corporation (ref. 4), General Precision, Inc. (ref. 5), and the United

States Naval Research Laboratory (refs. 6 to 8). The best backscattering information of near-vertical incidence that Moore cites was obtained by Sandia Corporation (refs. 9 and 10), but he further states that in all cases, spotty frequency coverage was obtained.

Moore describes ground return in terms of a differential cross sectional area, σ^0 , which represents the scattering cross section per unit area and which is designed to eliminate the total cross section, σ , of a large illuminated patch of ground determined by such system parameters as pulse width and beamwidth and operational mode. The backscattering coefficient used in this report differs from Moore's usage, for Moore does not use the projected area of the radar pulse packet; i.e., Moore's σ^0 is larger than that seen by the radar along the LOS by the sine of the depression angle.

In this report, the term "backscattering coefficient" is defined in units of scattering cross section per unit area and not as the ratio of the power reflected by an area to the energy incident on that area along a ray between the radar and the reflecting area.

4.3 BACKSCATTERING COEFFICIENT

The backscattering coefficient, σ_0 , can be described in terms of the radar equation and the assumption that the power across the antenna azimuthal beam is constant as follows:

$$P_R = \frac{P_t G^2 \lambda^2 \sigma_0 A_e}{(4\pi)^3 R_s^4} \quad (4-3)$$

where

P_R is the power received

P_t is the power transmitted

G is the antenna gain

λ is the radiated wavelength

Solving for the backscattering coefficient,

$$\sigma_0 = \frac{P_R (4\pi)^3 R_s^4}{P_t G^2 \lambda^2 A_e} \quad (4-4)$$

and substituting for A_e ,

$$\sigma_0 = \frac{P_R^2 (4\pi)^3 R_s^3}{P_t G^2 \lambda^2 \phi c \tau \tan \theta} \quad (4-5)$$

further substitution that

$$R_s = \frac{h}{\sin \theta}$$
$$\sigma_0 = \frac{P_R^2 (4\pi)^3 h^3 \csc^4 \theta \cos \theta}{P_t G^2 \lambda^2 \phi c \tau} \quad (4-6)$$

Equation (4-6) shows that for a constant backscattering coefficient from identical type terrains to obtain a constant received power, P_R , the antenna gain must be a function of depression or radar aspect angle, θ ; i.e.,

$$G^2(\theta) = G_0^2 \csc^4 \theta \cos \theta \quad (4-7)$$

or

$$G(\theta) = G_0 \csc^2 \theta \cos^{1/2} \theta \quad (4-8)$$

This type of elevation angle gain variation is the frequently used gain pattern of a SLR. Further discussion of antenna gain is included in other sections of this report.

An illustration of the variation in the backscattering coefficient σ_0 as a function of terrain and aspect angle (the depression angle from horizontal) is repeated in figure 4-3 (ref. 7). Figure 4-3 represents data from an airborne SLR operating at X band and shows that while terrain with heavy vegetation may have a backscattering coefficient of -10 decibels, variations about this value of approximately 4 decibels can be expected depending on what the radar "sees". To reiterate, then, the backscattered energy is a function of aspect angle, which is in turn a function of the antenna pattern in azimuth and elevation.

By the use of the above mentioned concepts, it is possible to describe a calibration method which is related to the backscattering coefficient, σ_0 . This implies that the parameters of equation (4-6) are known or can be measured in order to determine σ_0 .

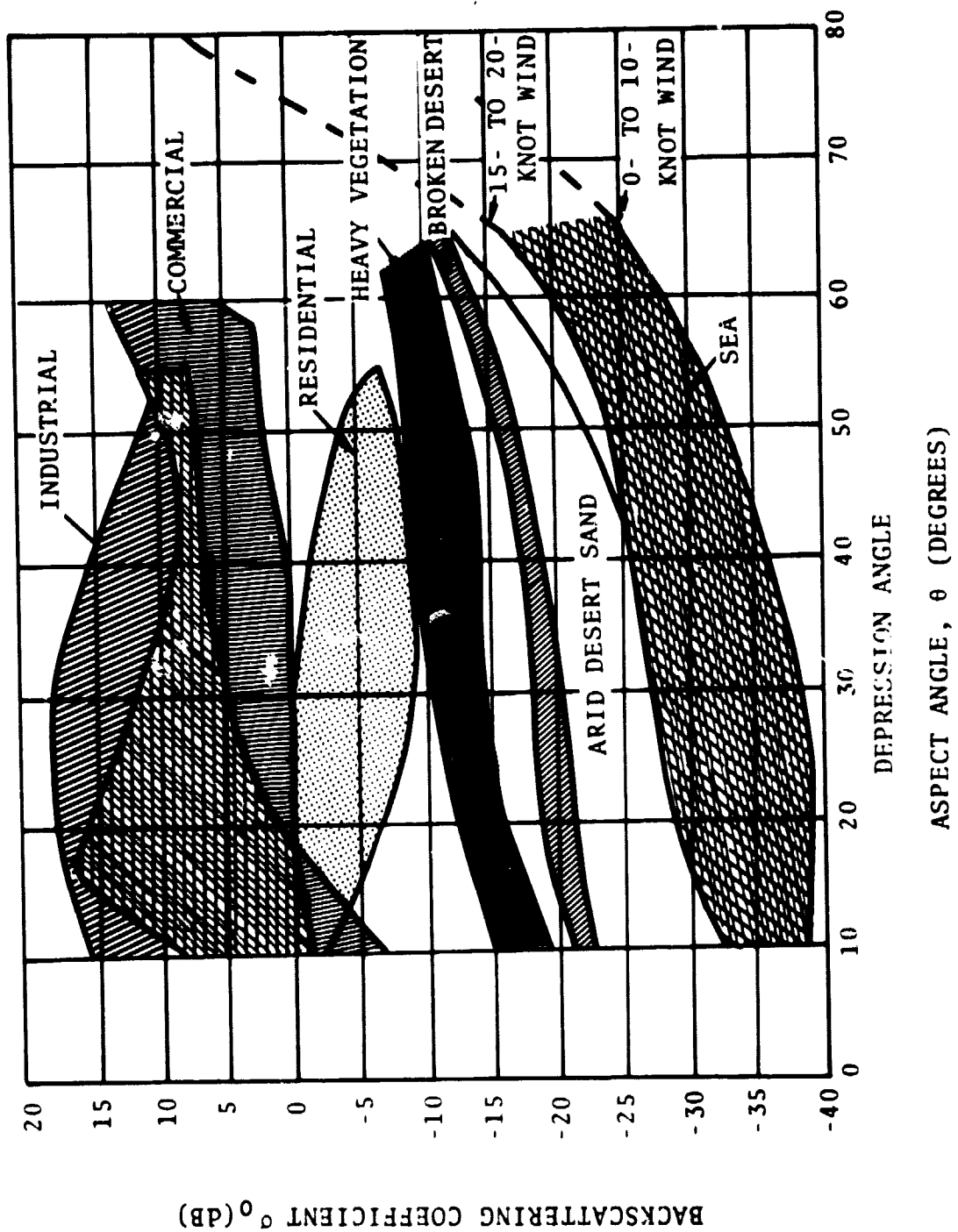


Figure 4-3. - Terrain return data.

5. TRANSFER FUNCTIONS

The transfer functions of all devices through which the radar mapping information passes must be accounted for if the calibration of a SLR is to be achieved. These various transfer functions are illustrated in figure 5-1 beginning with a radio frequency (rf) input to the receiver.

From figure 5-1, it can be seen that the receiver transfer function is but one element in a series of transfer functions. Others include the transfer functions of the recorder CRT, the radar data film, the optical correlator, the film maps, a microdensitometer, an analog-to-digital converter and a magnetic tape. The use of the above mentioned devices is discussed below.

5.1 RECEIVER

The receiver rf input versus video output voltage transfer function must be known in the calibration of a SLR. This transfer function is, in general, a non-linear curve as shown in figure 5-1. Ideally, the receiver transfer function would be linear which would allow only a single known input signal level for calibration. Since linear related signals produce nonlinear output voltages, multiple input signals must be used to obtain the transfer function curve. This non-linearity of the input-output receiver transfer function must be compensated for in the data processing.

5.2 RECORDER CRT

The receiver video is a bipolar voltage that is used to intensity modulate one or more CRT's within the recorder. This CRT(s) has an ambient light output, with no modulation, as a result of a direct current (dc) bias voltage being applied. The

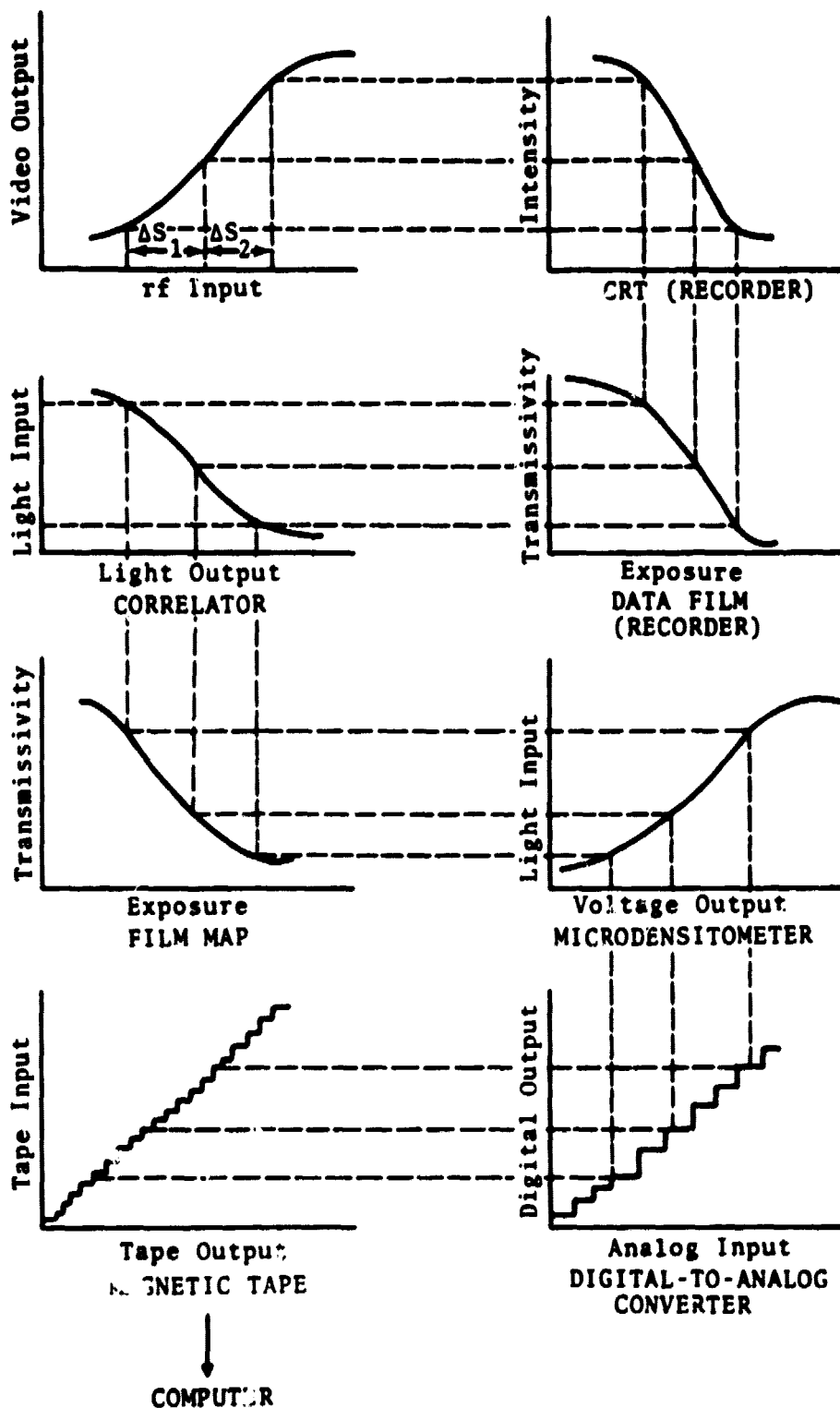


Figure 5-1. - Transfer characteristics of elements in a coherent SLR system.

bipolar video produces a light output that varies in intensity as a function of target backscatter and range. The dynamic range of the CRT is such that as many as 20 levels of light output can be observed by the recorder data film.

5.3 RECORDER DATA FILM

The recorder data film is exposed by the light output from the recorder CRT. The variations in exposure are also a function of target backscatter and range. The maximum CRT light output should be adjusted so that when the film is developed this maximum CRT light output produces a film density near or equal to 2.0, which corresponds to a transmissivity of 1.0 percent. The relationship between density and light transmissivity (ref. 11) is,

$$D = \log \left[(I) \left(\frac{1}{\tau} \right) \right] \quad (5-1)$$

where,

D is the film density

I is the light intensity on the film and

τ is the film transmissivity

that is,

<u>Density</u>	<u>Percent Transmissivity</u>
0.0	100.0
0.1	79.4
0.2	63.1
0.3	50.1
0.4	39.8
0.5	31.6
0.6	25.1
0.7	20.0
0.8	15.8
0.9	12.6
1.0	10.0
1.1	7.9
1.2	6.3
1.3	5.0
1.4	4.0
1.5	3.2
1.6	2.5
1.7	2.0
1.8	1.6
1.9	1.3
2.0	1.0

A standard photographic calibration density wedge should be exposed on the data film so that the transfer function can be determined. The data film will contain target information in the form of an optical grating corresponding in length, by a scaling factor, to the physical antenna beamwidth in the azimuth direction. This optical grating data film is used in a monochromatic optical correlator/processor to produce the film map.

5.4 OPTICAL CORRELATOR/PROCESSOR

The optical correlator/processor is the device used to produce the film map by imaging the data film through an optical system which is depicted in figure 5-2. The optical system consists of the following elements: a coherent light source, a collimating lens, the data film, a conical lens, a cylindrical lens, a field or integrating lens, an output slit and the output map film. The action of these elements in the optical correlator/processor is explained in figure 5-2. The output map film is the radar derived image of the terrain illuminated by the radar beam. The processes involved in obtaining a recognizable output map film by a SLR are shown in figure 5-3.

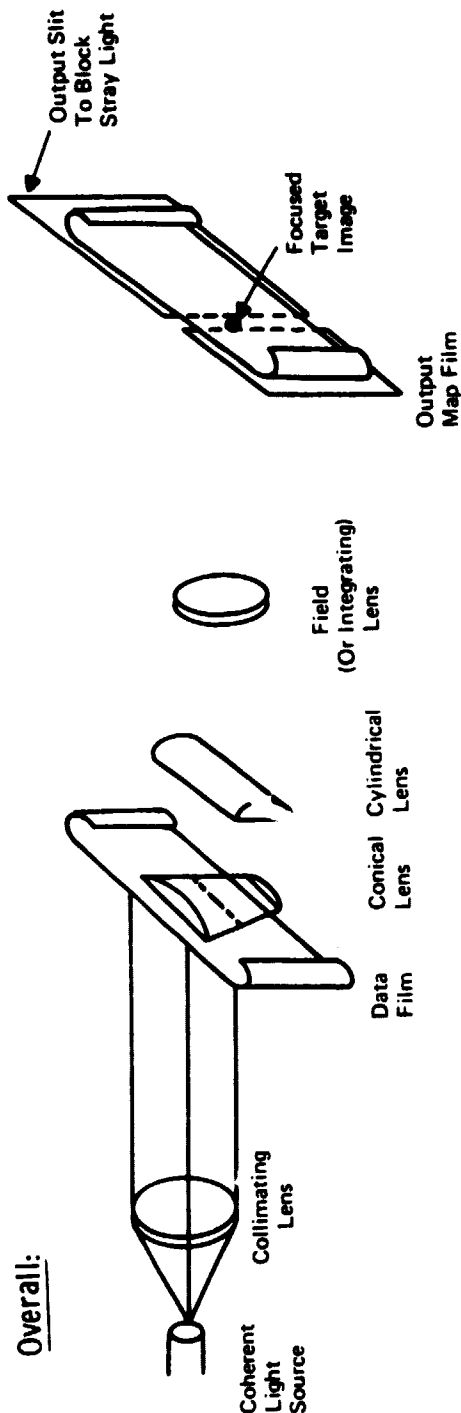
5.5 OUTPUT MAP FILM

The output map film from the optical correlator/processor must be developed by a chemical developing process. This output map film has 8 to 10 discernible grey levels, which must be converted to another information form for reduction by yet another processing technique. One such technique is using a microdensitometer to sweep an area of interest in the output map film.

5.6 MICRODENSITOMETER

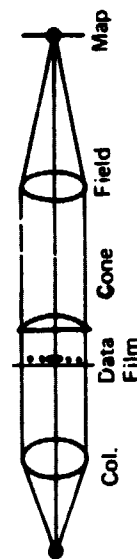
A microdensitometer (MD) is a device which has the capability of viewing a very small portion of the map film. In this viewing process, an optical aperture, which is small in comparison to the image of a point target is scanned across the map film. This scanning operation of the microdensitometer aperture may be accomplished by an operator or could be programmed to sweep an area of map film in some ordered scan pattern. The operator can use the signal amplitude directly by noting the various signal levels recorded from different

Overall:



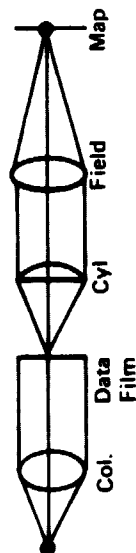
- Collimating Lens Makes Light Rays Parallel at Data Film Plane.
- Conical Lens Compensates for Range-Dependent Focal Length of Holograms.
- Cylinder Lens Focuses in Range Direction Since 1-D Hologram does not Range Focus.
- Field Lens Shortens Length of Processor because Hologram Focal Length Very long.
- Output Slit Blocks Stray Light from Output Film.

Azimuth:



Points along Hologram are Integrated

Range:



Points in Range are just Refocused in Output Plane with no Integration

S73-0085-V-9

Figure 5-2. - Typical optical correlator/processor.

The diagram illustrates the architecture of a Doppler radar system, organized into several functional blocks:

- Antenna and Receiver Section:**
 - Ant Control** and **Chutter Tracker** are connected to the **Antenna** (represented by a dish icon).
 - The **Antenna** feeds into the **Coherent Receiver**.
- Coherent Processing Section:**
 - The **Coherent Receiver** is connected to the **Coherent PULSED XMITTR** (Transmitter).
 - The **Coherent PULSED XMITTR** is connected to the **Stalo** (Stable Oscillator).
- Reference and Compensation Section:**
 - The **Coherent PULSED XMITTR** also feeds into the **Reference Gen**.
 - The **Reference Gen** is connected to the **Doppler Offset Gen** and the **Motion Compensation** block.
- Detector and Video Section:**
 - The **Coherent Receiver** feeds into the **Synchronous Detector**.
 - The **Synchronous Detector** outputs **Bipolar Video** to the **CRT or Laser Film Recorder**.
 - The **CRT or Laser Film Recorder** also receives **Velocity Analog** input.
- Optical Processor Section:**
 - The **CRT or Laser Film Recorder** feeds into the **Expose Data Film**.
 - The **Expose Data Film** feeds into the **Chemical Process**.
 - The **Chemical Process** feeds into the **Optical Correlator**.
 - The **Optical Correlator** also receives **Velocity Analog** input.
 - The **Optical Correlator** feeds into the **Expose Output Film**.
 - The **Expose Output Film** feeds into the **Chemical Process**.
 - The **Chemical Process** feeds into the **Viewing Station Output Film**.

5-7

target types. If a programmed scan pattern is used, target amplitude and aperture position must be recorded for each area of interest.

A typical scan pattern for the aperture of the MD is to scan a line across the film in the x-direction, then move over a distance, Δy , and repeat the x-direction scan. This scanning process is repeated a number of times, n , until the area of interest is completely scanned. The position of the aperture, in x and y coordinates, as well as the voltage amplitude from the MD, must be recorded. One method is to record x_n , y_n and amplitude in digital format on magnetic tape.

5.7 ANALOG-TO-DIGITAL CONVERTER

The analog-to-digital converter (ADC) quantizes the analog voltage from the microdensitometer, and outputs this voltage in a digital format. The clock rate required for this ADC will depend on the x-direction sweep rate of the MD. It is anticipated that the clock frequency will be in the kilohertz region. For example, if the x-direction line has 4000 elements scanned once per second and each element is sampled twice, the clock frequency would be 8000 hertz. If there are eight to ten distinct levels of grey on the map film which is viewed by the MD, then three to four bits are required to quantize the analog information into digital information. This quantized map film data is stored on magnetic tape along with quantized information on the x-y location of the MD aperture. ADC's must be used to encode these x and y locations in digital format.

5.8 DIGITAL MAGNETIC TAPE RECORDING

The format for digital magnetic tape recording will be determined by the format of the computer which reduces the data. For example, the bit packing density may be 800 bits per inch

to be computer compatible. The tape will have recorded information on the MD aperture x-y position, target return amplitude, and perhaps geometric coordinates of the target if absolute target location is required. If absolute target location is desired, then latitude/longitude information must be preserved by the data film and transferred to the map film.

6. COMPUTER DATA PROCESSING

It is anticipated that the radar mapping information will be stored on magnetic tape and will be used as the input to a computer. The software for radar data processing will include descriptions of the following:

- The antenna elevation and azimuth patterns
- The transmitter pulse shape and duration
- The transfer functions of all elements from the receiver through the microdensitometer
- The input signal level to the receiver versus signal level out of the microdensitometer
- Equation (4-6) for calculating backscattering coefficient
- The location of the microdensitometer aperture

By processing the radar mapping data and knowing the above mentioned parameters, it will be possible to use the computer to determine the backscattering coefficient for any mapped target.

If computer data processing is not desired other analog/operator calibration can be used.

7. CALIBRATION METHODS

To calibrate a SLR, it is necessary to define the meaning of the term "calibration". As herein defined, the calibration of a SLR is the ability to relate known reference levels to unknown radar backscatter by the use of one or more calibration techniques.

Calibration of a SLR requires knowledge of (1) the individual transfer functions of each device through which the radar mapping information passes, or (2) an overall transfer function of several devices in the calibration chain. These items in the chain (described in section 5.) are typical of a SLR employing film recording techniques. Other configurations could be envisioned, but this example is adequate to address the problems encountered.

7.1 SIMULATED TARGETS

One method of calibrating a SLR from the receiver to the microdensitometer (see figure 5-1) is to feed a known signal level into the receiver input port. This calibration signal must be frequency modulated in a manner to simulate real targets and must be recorded on the recorder data film. Typically, this frequency modulation (FM) would be linear for a few hundred hertz over a period of a second. Signal power levels of -100 dBm to -30 dBm would probably be required to obtain the total transfer function characteristics from the receiver input to the output of the microdensitometer. While this method may be easily accomplished, there are serious drawbacks in that it only partially defines the SLR target response. A better and more highly recommended method would be that of a calibrated test range.

7.2 CALIBRATION TEST RANGE

At this time, as far as is known, all radar ranges have been sponsored by the armed forces and have reflected their need for resolution, detection and identification of small targets (a truck, for instance) in the midst of terrain clutter. The needs of an earth resources program, however, differ in many respects. While good radar resolution will assist in many facets of earth resources studies, the need for a system with wide dynamic range, excellent image smoothing, built-in calibration and related capabilities are equally important. Since these needs require a different sort of radar test range, the following sections provide description for a test range that should prove useful in earth resources studies.

7.2.1 DISTRIBUTED TARGET RESOLUTION

Many radar systems have different transfer functions for point and distributed targets. Therefore, both types of targets with a range of reflectivities should be provided. The point targets are relatively conventional; a set of carefully sized reflectors will do. However, distributed targets require more thought. These targets should have a constant reflectivity over each target area and should not change appreciably with the passage of time. Large patches of crushed and sized rock have been suggested. Whatever the materials used, the target should be large enough in extent to contain at least five or six resolvable elements of the worst resolution expected of any radar to be used on it. In this manner, there is some assurance that the proper target is being observed on the radar imagery. Possibly, the most direct approach to measurement of distributed target resolution would be to taper the target shape to point to allow accurate resolution measurement, and to provide several reflective materials in different patches for a multicontrast target, much the same as in optics.

7.2.2 SYSTEM DYNAMIC RANGE MEASUREMENT

A relatively direct measurement of system dynamic range can be made by imaging a series of known radar reflectors at the same time. Then the system response can be measured for each reflector and the system response can be determined. Care must be taken to fashion the pattern of reflectors so that there can be no doubt about the location and identity of each reflector in the pattern. In addition, the possibility of multipath signals should be minimized by careful design.

Above all, any radar test range must be clearly visible and unambiguous on the radar imagery. There should be no doubt whatsoever in the mind of the interpreter concerning which resolution target or which contrast area is being examined. As a result of this and the preceding characteristics, it is suggested that a radar calibration site be constructed as shown in figure 7-1. This circular pattern allows for distributed and point target resolution testing, with variable contrast distributed targets. In addition, a complete system dynamic range measurement is available on each radar image.

Variable contrast distributed targets are formed by the pie-shaped segments of material having different particle sizes. In the example shown, all possible combinations of four different reflective surfaces are present, and the resolution on any contrast set can be measured by determining the distance toward the center that the pie segment can be distinguished, either visually or by an arbitrary power level standard.

Point target resolution targets are arranged rather conventionally serving to mark the corners of the site.

System dynamic range measurement is provided by the circle of graduated reflectors which also mark the pie sectors. These

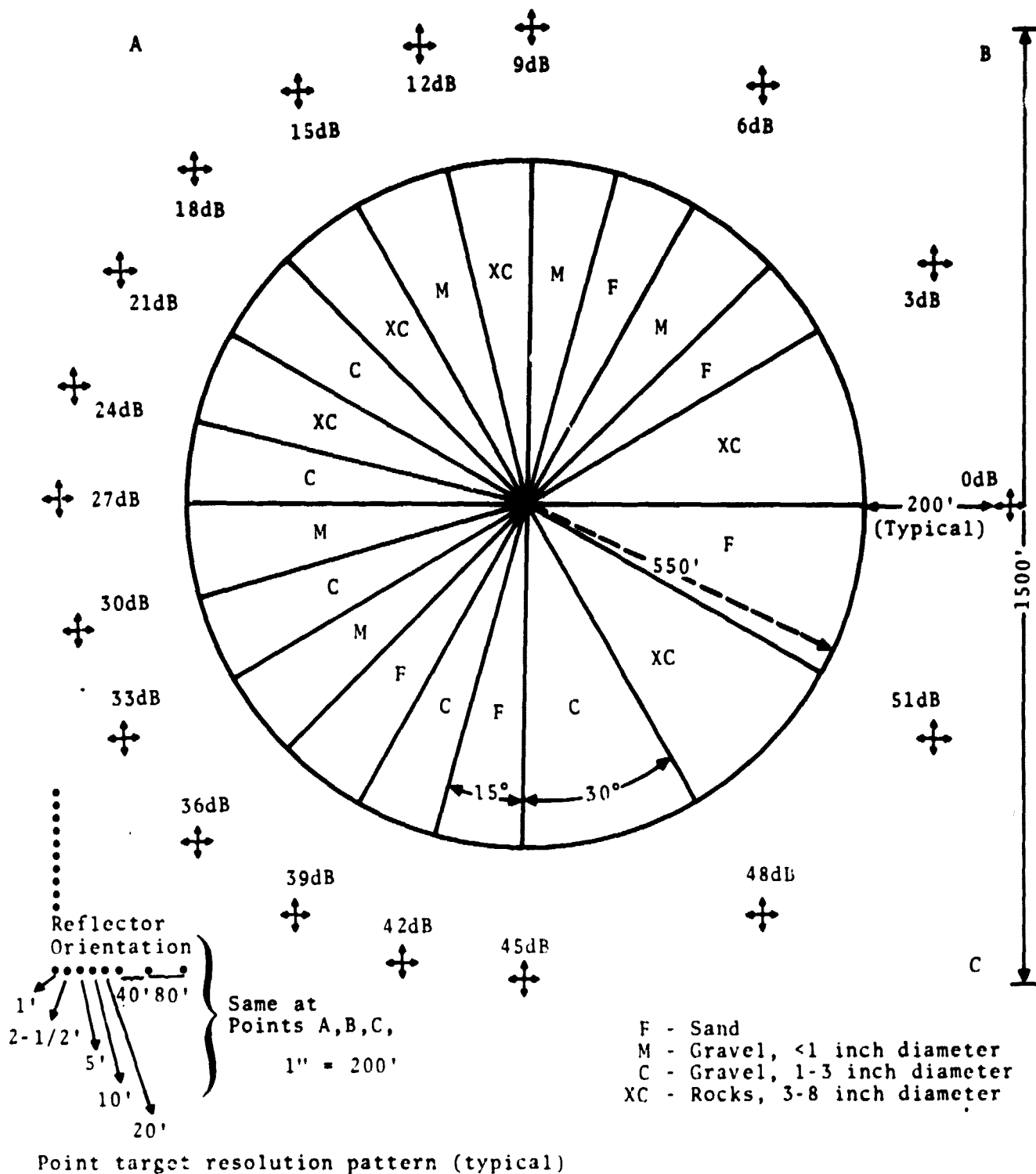


Figure 7-1. - Radar Calibration Test Range.

reflectors should have a considerably larger dynamic range than is expected of any current radar to avoid their immediate obsolescence. The pattern shown is for a 51 dB range of reflectivities at X band, and representative sizes of luneberg lens reflectors for such a range of reflectivities are shown below:

σ_0	σ	Reflector Radius
dB	m^2	m
0	1	.10
10	10	.17
20	100	.30
30	1000	.54
40	10000	.96
50	100000	1.70

The radar calibration range described here would require four each of eighteen different sizes of calibrated reflectors, together with sixty point target resolution reflectors. Such an arrangement will permit omnidirectional coverage without the need for readjustment of the reflectors, which is a desirable characteristic since adjustable reflectors nearly always lead to some doubt in the minds of investigators concerning what the adjustment was on test day. The type of reflector recommended for this test range is the luneberg lens with a 90° cap. This reflector has the small physical dimensions required for the resolution targets and has a high reflectivity which is nearly constant over a 90° solid angle making it desirable for system response measurement. Thus, each dynamic range reflector site should consist of four reflectors of the same size, arranged back-to-back in pairs. Since the radar reflectivity of the ground around the reflectors will contribute to the received signal, it is desirable to have the area around the reflectors as smooth and level as practicable. It is suggested that the reflectors all face parallel to the sides of the square test

pattern, as indicated in the figure, and that each reflector face upward at an angle of approximately 40° from the horizontal in order to provide adequate vertical coverage. Reflectors having a 10 m^2 radar cross section at 10 Gc are recommended for the resolution targets for 10-foot spacing and greater, with 1 m^2 targets for less than 10-foot spacing. It is apparent that all of the reflectors used for calibration targets must be measured for reflectivity pattern after fabrication, and that the reflector pattern and location should be made available to each investigator using the radar imagery.

The sand and gravel beds constituting the distributed target pattern should be laid on top of the ground, rather than set into the soil. This will minimize changes due to standing water or silt deposition. A bed thickness of 1 foot will be adequate for all except the $3/8$ inch rocks, which may have to be 1-1/2 feet thick to provide a complete ground cover. The perimeter of the circle can be of any desired restraining material, such as a ridge of dirt, but it must have adequate provisions for water drainage. The sector dividers, however, should be made of, or covered with, an absorbent material such as Eccosorb. This will prevent reflections from the dividers or edge effects from interfering with the resolution measurement process.

A pattern such as this offers several advantages to the radar system user:

1. Distributed target multicontrast resolution test pattern with essentially infinite variable resolution capability (from 0 to 300 feet).
2. Complete radar system dynamic range measurement and calibration over a 50 dB range and limited capability for distributed target dynamic range testing.

3. Point target resolution test patterns of spacing down to 1 foot.

4. Short term geometric fidelity test capability.

All of these system measurements are available on each and every radar image of the test pattern, without imposing critical limitations on flight path position or requiring coordinated ground operations.

7.2.3 PLANNING CONSIDERATIONS

When designing and constructing a radar test range, it might be well to consider the various difficulties which may be encountered. For example, it may be difficult to:

1. Place the test range where no nearby objects or terrain can cause confusion about the location of the test range or its boundaries.
2. Arrange the test pattern so that it is completely unambiguous on the imagery.
3. Design the test range to eliminate the need for coordinated ground activity, i.e., no adjustments to reflector positions before a flight, etc. A range with fixed, well-known, omnidirectional characteristics is highly desirable.
4. Construct the range to minimize the effects of time and weather upon its response.
5. Select a site for the test range which allows using aircraft sufficient airspace to image the site freely from more than one side. Mountains, airport control areas, and airways can cause varying amounts of interference with the flight of the test aircraft.
6. Make certain that the test site is not open to the casual visitor.

7. Design the test pattern to yield a maximum of information with a minimum of flights and to be flexible enough to serve radar systems yet to be acquired.

8. CONCLUSIONS

It is possible to calibrate a SLR in terms of backscattering coefficient. Calibration can be obtained by the use of:

1. Know rf input levels injected into the receiver,
2. A reflector range,
3. An equation to calculate backscattering coefficient, σ_o , that is,

$$\sigma_o = \frac{P_R 2(4\pi)^3 h^3 \csc^4 \theta \cos \theta}{P_t G(\theta)^2 \lambda^2 \phi c\tau} \quad (8-1)$$

4. A digital computer with appropriate software, or
5. An operator to observe the output level of a microdensitometer whose aperture is placed over film areas of interest.

9. REFERENCES

1. Moore, R. K.: "Ground Echo," in Radar Handbook, Ch. 25. M. I. Skolnik, ed. New York: McGraw-Hill, 1970.
2. Clapp, R. E.: "A Theoretical and Experimental Study of Radar Ground Return." MIT Radiation Laboratory Rept. 6024, April 1946.
3. George, T. S.: "Fluctuations of Ground Clutter Return in Airborne Radar Equipment." Proc. IEE, vol. 99 (Apr. 1952), pp. 92-96.
4. Reitz, E. A., et al.: "Radar Terrain Return Study, Final Report: Measurements of Terrain Backscattering Coefficients with an X-Band Radar." Goodyear Aerospace Corp. Rept., GERA-463, 1959.
5. Campbell, J. P.: "Backscattering Characteristics of Land and Sea at X-Band." Proc. Nat. Conf. Aeron. Electron., May 1958.
6. MacDonald, F. C.: "The Correlation of Radar Sea Clutter on Vertical and Horizontal Polarization with Wave Height and Slope." IRE Conv. Record, vol. 4, pt. 1 (1956), pp. 29-32.
7. Ament, W.; MacDonald, F.; and Shewbridge, R.: "Radar Terrain Reflections for Several Polarizations and Frequencies." Trans. 1959 Symp. Radar Return, pt. 2, May 11-12, 1959.
8. Grant, C. R.; and Yaplee, B. S.: "Back Scattering from Water and Land Surface at Centimeter and Millimeter Wavelengths." Proc. IRE, vol. 45 (July 1957), pp. 976-982.
9. Edison, A. R.; Moore, R. K.; and Warner, B. D.: "Radar Return at Near-vertical Incidence." Univ. New Mex. Eng. Expt. Sta., Tech. Rept. EE-24, Sept. 1959.
10. Bidwell, C. H.; Gragg, D. M.; and Williams, C. S.: "Radar Return from the Vertical for Ground and Water Surface." Sandia Corp. Monograph SCR-107, April 1960.

11. "Photographic Reference Handbook." Hycon Mfg. Company,
1961.
12. Skolnik, M. I.: "Introduction to Radar Systems." McGraw-
Hill, 1962.
13. "Imaging Radars for Earth Resources." Technical Report.
LEC/HASD 649D-21-006, July, 1969.